CHEMISTRY
A EUROPEAN JOURNAL

DOI: 10.1002/chem.201001911

Kinetic Data for the Transmetalation/Reductive Elimination in Palladium-Catalyzed Suzuki–Miyaura Reactions: Unexpected Triple Role of Hydroxide Ions Used as Base

Christian Amatore,* Anny Jutand,* and Gaëtan Le Duc[a]

Dedicated to Professor Marc Julia

Abstract: The mechanism of the reaction of *trans*-[ArPdX(PPh_3)$_2$] (Ar = *p*-Z-C_6H_4; Z = CN, F, H; X = I, Br, Cl) with Ar′B(OH)$_2$ (Ar′ = *p*-Z′-C_6H_4; Z′ = CN, H, OMe) has been established in DMF in the presence of the base OH^- in the context of real palladium-catalyzed Suzuki–Miyaura reactions. The formation of the cross-coupling product ArAr′ and [$Pd^0(PPh_3)_3$] has been followed through the application of electrochemical techniques. Kinetic data have been obtained for the first time, with determination of the observed rate constant, k_{obs}, of the overall reaction. *trans*-[ArPdX(PPh_3)$_2$] is not reactive in the absence of the base. The base OH^- plays three roles. It favors the reaction: 1) by formation of *trans*-[ArPd(OH)(PPh_3)$_2$], a key complex which, in contrast to *trans*-[ArPdX(PPh_3)$_2$], reacts with Ar′B(OH)$_2$ (rate-determining transmetalation), and 2) by unexpected promotion of the reductive elimination from the intermediate *trans*-[ArPdAr′(PPh_3)$_2$], which generates ArAr′ and a Pd^0 species. Conversely, the base OH^- disfavors the reaction by formation of the unreactive anionic Ar′B(OH)$_3^-$. As a consequence of these antagonistic effects of OH^-, the overall reactivity is controlled by the concentration of OH^- and passes through a maximum as the concentration of OH^- is increased. Therefore, the base favors the rate-determining transmetalation and unexpectedly also the reductive elimination.

Keywords: arylboronic acid · base · kinetics · palladium · transmetalation

Introduction

The palladium-catalyzed Suzuki–Miyaura cross-coupling of aryl halides and arylboronic acids[1,2] takes place in the presence of a base (e.g., $Ba(OH)_2$, NaOH, K_3PO_4, Na_2CO_3, Cs_2CO_3, $NaHCO_3$, NaOAc)[3] (Scheme 1). The base is crucial, but up to now its role has never been fully rationalized.[1–4]

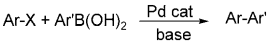

Scheme 1.

In a first approach, one may consider the first step of the catalytic cycle to be an oxidative addition of the aryl halide ArX to a Pd^0 complex [Pd^0L_n] to afford [ArPdXL_n]. This complex then reacts with the arylboronic acid Ar′B(OH)$_2$ in a transmetalation step to form [ArPdAr′L_n]. The catalytic cycle is completed by a reductive elimination, which generates the coupling product ArAr′ and the Pd^0 catalyst. Based on such a hypothetical framework, the reactions should proceed in the absence of a base, since no proton transfer is required at any stage. However, a base is required for all such catalytic reactions.[1–3] The role of the base (RO^-) was first ascribed to the formation of aryl hydroxyborates Ar′B(OH)$_2$(OR)$^-$ (R = H,[4a] Me[2f]) or trialkyl borates,[4b] which were considered as being more nucleophilic, and hence more reactive with [ArPdXL_n] in the transmetalation step (step b in Scheme 2). Another role of the base (e.g., with R = Me, MeCO) was postulated by Miyaura, Suzuki et al. through invoking the formation of [ArPd(OR)L_2] (L = PPh_3), the transmetalation of which with Ar′B(OH)$_2$ should be favored by the oxophilicity of the boron center (step c in Scheme 2).[2c,5] They indeed observed that the reaction of *trans*-[(Ph)PdBr(PPh_3)$_2$] with (R′O)$_2$B–B(OR′)$_2$ was acceler-

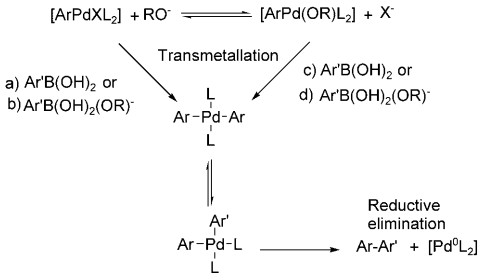

Scheme 2. Postulated mechanisms for the transmetalation/reductive elimination.

[a] Dr. C. Amatore, Dr. A. Jutand, G. Le Duc
Département de Chimie, Ecole normale Supérieure
UMR CNRS-ENS-UPMC 8640
24 Rue Lhomond, 75231 Paris Cedex 5 (France)
Fax: (+33) 144322402
E-mail: christian.amatore@ens.fr
Anny.Jutand@ens.fr

ated in the presence of acetate ions (KOAc in DMSO),[2c] and that this generated *trans*-[(Ph)Pd(OAc)(PPh_3)$_2$] by Br/OAc exchange.[6] [(Ph)Pd(OH)(PPh_3)$_2$] formed by Br/OH exchange in [(Ph)PdBr(PPh_3)$_2$] was also proposed as a reactive intermediate with alkylboranes by Soderquist et al.[4b] A dual role of the base, that is, the formation of [ArPd(OR)L_2] and Ar′B(OH)$_2$(OR)$^-$, was also considered (step d in Scheme 2).[2f] DFT calculations on model molecules have established that the transmetalation of $PhB(OH)_2$ with [(Ph)PdBrL_2] "can take place smoothly through reaction of [(Ph)PdBrL_2] with $PhB(OH)_3^-$" (step b in Scheme 2, L = PH_3,[7a] PPh_3[7b]) "or through reaction of [(Ph)Pd(OH)(PH_3)$_2$] with $PhB(OH)_2$ in the absence of the base" (step c in Scheme 2).[7a]

A catalytic cycle is a succession of elemental steps involving organometallic species, with the concentrations of these species remaining low compared to those of the reagents. To establish the mechanism of a catalytic cycle, one needs to investigate the rate and mechanism of each successive step under conditions close to those of the catalytic reaction. The rate and mechanism of the first step of the catalytic cycle, that is, the formation of *trans*-[ArPdX(PPh_3)$_2$] (X = I, Br, Cl) by oxidative addition of ArX to [Pd^0(PPh_3)$_2$], are now well-documented.[8] The second step of the catalytic cycle concerns the reaction of Ar′B(OH)$_2$ with *trans*-[ArPdX(PPh_3)$_2$] (termed transmetalation), the role of the base in which is still not completely understood (vide supra). The present work is devoted to elucidating the role of the base. Encouraged by some qualitative results on the reaction between *p*-NC-C_6H_4-B(OH)$_2$ and [(*p*-Z-C_6H_4)Pd(OH)(PPh_3)$_2$] (Z = H, OMe) obtained during our mechanistic work on the palladium-catalyzed homocoupling of arylboronic acids in the presence of dioxygen,[9] and in the absence of any kinetic data on the transmetalation step in the literature, we decided to investigate the kinetics of the reaction of arylboronic acids Ar′B(OH)$_2$ with isolated *trans*-[ArPdX(PPh_3)$_2$] complexes (X = I, Br, Cl)[10] in the presence of a base such as OH^-. The investigations presented and discussed in the present work have been performed not under stoichiometric conditions of reagents with respect to *trans*-[ArPdX(PPh_3)$_2$] complexes, but always in the presence of large excesses of Ar′B(OH)$_2$ (from 10 to 30 equiv) and base, to mimic the catalytic reaction conditions (from 10 to 3.3 mol% catalyst, respectively). The present experiments were thus conducted under conditions that were perfectly representative of one cycle of a real catalytic sequence. The only difference with respect to a real catalytic situation that may be invoked concerns the fact that we started the catalytic cycle with [ArPdXL_2], that is, after the oxidative addition step. This is valid when the oxidative addition is fast, as is the case with most aryl bromides or aryl iodides. The oxidative addition may be the rate-determining step for aryl chlorides, but then the kinetics of the system would relate to the following reactions. From our point of view, the main unknowns about the title reaction relate to the steps occurring after the oxidative addition, and especially to the previously poorly understood role of the base.

It is established herein that the base OH^- plays a triple role: 1) formation of [ArPd(OH)(PPh_3)$_2$] as the reactive species involved in the rate-determining transmetalation step, 2) formation of unreactive Ar′B(OH)$_3^-$ by reaction of OH^- with ArB(OH)$_2$, and 3) quite unexpectedly, acceleration of the reductive elimination step by reaction of OH^- with the intermediate *trans*-[ArPdAr′(PPh_3)$_2$] complex.

Results and Discussion

Since most reactions of *trans*-[ArPdX(PPh_3)$_2$] with Ar′B(OH)$_2$ in the presence of OH^- are too fast to be monitored by ^{1}H or ^{31}P NMR spectroscopy, we resorted to electrochemical techniques to follow the reactions, taking advantage of the fact that reduction or oxidation currents are proportional to the concentrations of the electroactive species.[11] It thus became possible: 1) to observe the reaction of Ar′B(OH)$_2$ with *trans*-[ArPdXL_2] (L = PPh_3; in the presence or absence of the base) through the evolution of the reduction current of the Pd^{II} complex, 2) to observe the formation of the intermediate [ArPdAr′L_2] (based on its reduction current) on the way to reductive elimination, 3) to observe and quantify the final Pd^0 complex (based on its oxidation current) that was formed after transmetalation/reductive elimination, and 4) to observe and quantify the formation of the cross-coupling product ArAr′ (based on its reduction current). DMF was selected as the solvent, and OH^- as a typical soluble base (introduced as nBu$_4$NOH, 1 M in methanol). Methanol and DMF are good solvents for Suzuki–Miyaura reactions.[1–3] As many reactions are catalyzed by [Pd^0(PPh_3)$_4$][1–3] (i.e., [Pd^0(PPh_3)$_3$] in solution in DMF[12]), the electrochemical monitoring of the reactions was performed in the presence of two equivalents of PPh_3 per palladium(II) to observe the formation of the stable complex [Pd^0(PPh_3)$_3$] after reductive elimination (Scheme 3). These selected con-

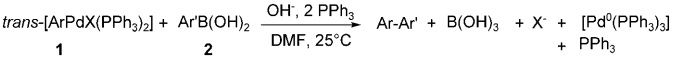

Scheme 3.

ditions for the electrochemical experiments were thus close to those of real catalytic reactions. Using the electrochemical techniques, we were able to follow the overall reaction in Scheme 3, that is, the transmetalation and/or reductive elimination steps, depending on their relative rates.

Tentative reactions of *trans*-[ArPdX(PPh_3)$_2$] with Ar′B(OH)$_2$ in the absence of a base: The isolated complex [(*p*-NC-C_6H_4)PdBr(PPh_3)$_2$] (1.9 mM; $\mathbf{1}_{CN,Br}$) in DMF (containing 0.3 M nBu$_4$NBF$_4$ as supporting electrolyte) was characterized by an irreversible reduction peak at $E^p_{R1} = -1.83$ V versus SCE in a cyclic voltammogram obtained at a fixed gold electrode (Figure 1a). A poorly defined oxidation peak characteristic of a Pd^0 complex was observed on the reverse

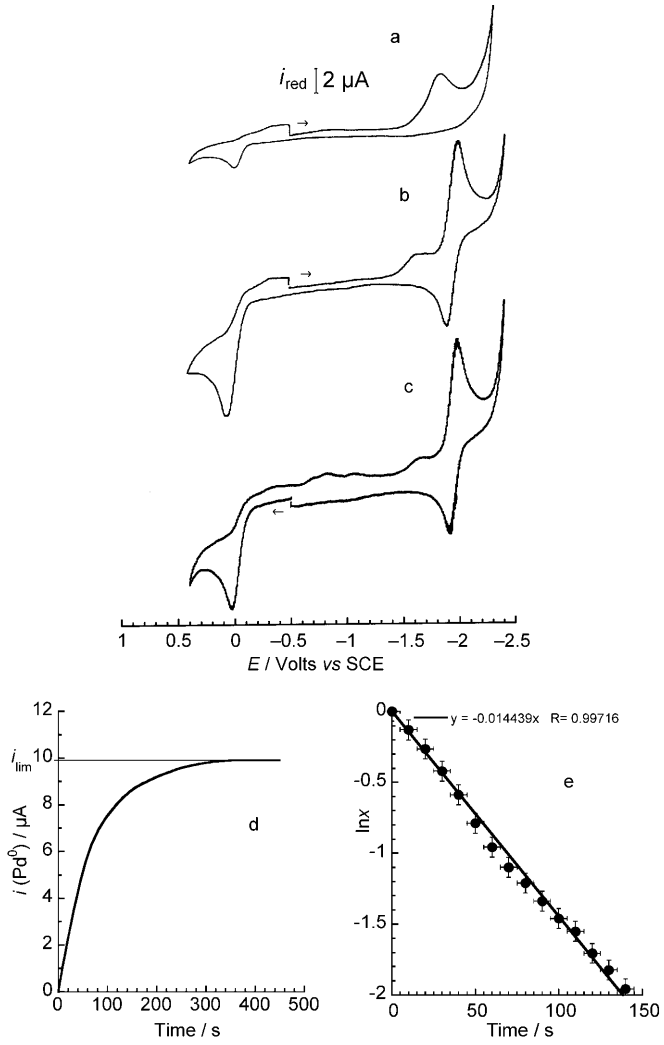

Figure 1. Cyclic voltammetry performed at a fixed gold disk electrode ($d=1$ mm) in DMF containing 0.3 M nBu_4NBF_4 at a scan rate of 0.5 V s^{-1} at 25 °C. a) Reduction of *trans*-[(*p*-NC-C_6H_4)PdBr(PPh_3)$_2$] ($\mathbf{1}_{CN,Br}$; 1.9 mM) in the presence of PPh_3 (3.8 mM). b) Reduction of *p*-NC-C_6H_4-Ph formed after 400 s by addition of $PhB(OH)_2$ (20 equiv) to $\mathbf{1}_{CN,Br}$, followed by OH^- (10 equiv). c) Oxidation of [$Pd^0(PPh_3)_3$] formed together with *p*-NC-C_6H_4-Ph as in b). d) Kinetics of the reaction of *trans*-[(*p*-NC-C_6H_4)PdBr(PPh_3)$_2$] ($\mathbf{1}_{CN,Br}$; 1.9 mM) with $PhB(OH)_2$ (20 equiv) in the presence of PPh_3 (2 equiv) and OH^- (10 equiv). Evolution of the oxidation current i of [$Pd^0(PPh_3)_3$] (proportional to its concentration) versus time. i was determined by chronoamperometry performed at a rotating gold disk electrode ($d=2$ mm) polarized at +0.05 V. e) Plot of ln x versus time: $x=(i_{lim}-i_t)/i_{lim}$; i_{lim}: final oxidation current of [$Pd^0(PPh_3)_3$]; i_t: oxidation current of [$Pd^0(PPh_3)_3$] at time t (see Figure 1d).

scan at $E^p_{O1}=+0.029$ V. Its oxidation peak current was amplified when the reduction of $\mathbf{1}_{CN,Br}$ was performed in the presence of two equivalents of PPh_3 (Figure 1a). As previously established, the reduction of $\mathbf{1}_{CN,Br}$ proceeds according to the mechanism reported in Scheme 4.[13] This allowed us to observe the fate of [(*p*-NC-C_6H_4)PdBr(PPh_3)$_2$] ($\mathbf{1}_{CN,Br}$) based on the evolution of its reduction peak current (proportional to its concentration) in the presence of Ar′$B(OH)_2$.

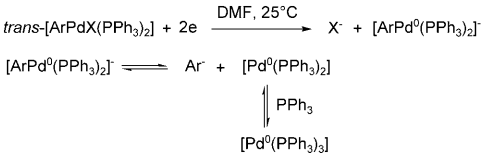

Scheme 4.

No reaction occurred when $PhB(OH)_2$ ($\mathbf{2}_H$; from 1 to 20 equiv) was added to $\mathbf{1}_{CN,Br}$ in the absence or presence of PPh_3 (2 equiv) at 25 °C. The reduction peak current of $\mathbf{1}_{CN,Br}$ did not vary even over long durations (up to 90 min), attesting to the absence of reaction under these experimental conditions (Scheme 5).

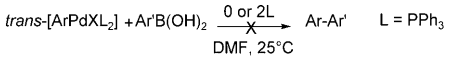

Scheme 5.

The situation changed drastically upon addition of the base OH^- (10 equiv). After a few minutes, the reduction peak of $\mathbf{1}_{CN,Br}$ was no longer observed when a voltammogram was measured towards reduction potentials (from −0.5 to +2.4 V; Figure 1b), but a new reversible reduction peak appeared at −2.01 V characteristic of the cross-coupling product *p*-NC-C_6H_4-C_6H_5, the identity of which was confirmed by addition of an authentic sample. An oxidation peak at +0.05 V characteristic of [$Pd^0(PPh_3)_3$][12] was observed when a voltammogram was first acquired by scanning towards oxidation potentials (from −0.5 to +0.6 V; Figure 1c). Similarly, no reaction took place between *trans*-[(C_6H_5)PdI(PPh_3)$_2$] (1.9 mM; $\mathbf{1}_{H,I}$) and *p*-MeO-C_6H_4-$B(OH)_2$ ($\mathbf{2}_{MeO}$; 10 equiv) within 8 h until the base OH^- was added.

Through these preliminary reactions, it was established that: 1) the presence of a base such as OH^- is required to induce the formation of the cross-coupling product, and 2) the electrochemical technique is adequate for following the reaction kinetics through monitoring the formation of the two products of the transmetalation/reductive elimination steps, namely [$Pd^0(PPh_3)_3$] and the coupling product ArAr′, which are formed in stoichiometric amounts and, more interestingly, at the same rate in the reductive elimination step (Scheme 2).

Kinetics of the reaction of *trans*-[ArPdX(PPh_3)$_2$] with Ar′$B(OH)_2$ in the presence of a base OH^-: To identify the role of the base and the mechanism leading to the formation of the coupling product ArAr′ (Scheme 6), the kinetics of

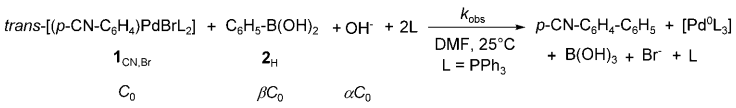

Scheme 6.

the formation of $[Pd^0(PPh_3)_3]$ during the reaction of $[(p\text{-NC-}C_6H_4)PdBr(PPh_3)_2]$ ($\mathbf{1}_{CN,Br}$; $C_0 = 1.9$ mM) with $PhB(OH)_2$ ($\mathbf{2}_H$; βC_0) in the presence of PPh_3 ($2\,C_0$) and OH^- (αC_0) was followed by chronoamperometry[11] in DMF. A rotating gold disk electrode was polarized at +0.05 V, the oxidation potential of $[Pd^0(PPh_3)_3]$. The oxidation current was zero before the addition of OH^-, attesting that no reaction took place between $\mathbf{1}_{CN,Br}$ and $\mathbf{2}_H$. After the addition of OH^- (αC_0), the oxidation current of $[Pd^0(PPh_3)_3]$ increased with time to reach a final constant value, i_{lim}, corresponding to the end of the reaction (Figure 1d, $\alpha = 10$, $\beta = 20$). During this time, the solution became yellow, which is characteristic of $[Pd^0(PPh_3)_3]$ in DMF.[12] At the end of the reaction (400 s), a voltammogram obtained at a fixed gold disk electrode by scanning first towards oxidation potentials exhibited the oxidation peak of $[Pd^0(PPh_3)_3]$ at +0.03 V (Figure 1c). The amount of $[Pd^0(PPh_3)_3]$ was determined from the increase in its oxidation peak current after the addition of a known amount of an authentic sample of $[Pd^0(PPh_3)_4]$. The yield of the reaction was 94% (Table 1). A voltammogram was also obtained by scanning towards reduction potentials, which showed that the cross-coupling product $p\text{-NC-}C_6H_4\text{-}C_6H_5$ had been formed, as attested by its reversible reduction peak at −2.01 V (Figure 1c). The amount of $p\text{-NC-}C_6H_4\text{-}C_6H_5$ formed in the reaction was determined on the basis of the increase in its reduction peak current after the addition of a known amount of an authentic sample. The yield of the reaction was 95% (Table 1), which exactly matched that of $[Pd^0(PPh_3)_3]$. The same kinetic curve (Figure 1d) was obtained when pre-mixed $\mathbf{2}_H$ ($20\,C_0$) and OH^- ($10\,C_0$) were added to $\mathbf{1}_{CN,Br}$ ($C_0 = 1.9$ mM).

Table 1. Yields of $[Pd^0(PPh_3)_3]$ and ArAr′ formed in the reaction of *trans*-$[(p\text{-Z-}C_6H_4)PdX(PPh_3)_2]$ (1.9 mM) with $p\text{-Z′-}C_6H_4\text{-}B(OH)_2$ (β equiv) in the presence of PPh_3 (2 equiv) and OH^- (α equiv) in DMF at 25 °C.

$[(p\text{-Z-}C_6H_4)PdXL_2]$ $\mathbf{1}_{Z,X}$	$p\text{-Z′-}C_6H_4\text{-}B(OH)_2$ $\mathbf{2}_{Z'}$ (β equiv)	OH^- α equiv	$[Pd^0L_3]$ Yield [%][a]	ArAr′ Yield [%][a]
$\mathbf{1}_{CN,Br}$	$\mathbf{2}_H$ (15)	10	99	99
$\mathbf{1}_{CN,Br}$	$\mathbf{2}_H$ (20)	10	94	95
$\mathbf{1}_{H,Br}$	$\mathbf{2}_H$ (20)	15	90	n.d.
$\mathbf{1}_{CN,Cl}$	$\mathbf{2}_H$ (20)	20	99	86
$\mathbf{1}_{CN,Br}$	$\mathbf{2}_{CN}$ (20)	15	92	94

[a] Yields are relative to $\mathbf{1}_{Z,X}$.

In most cases, a plot of $\ln x$ versus time was essentially linear up to 80% conversion (Figure 1e, vide infra; $x = (i_{lim} - i_t)/i_{lim}$; i_{lim}: final oxidation current of $[Pd^0(PPh_3)_3]$; i_t: oxidation current of $[Pd^0(PPh_3)_3]$ at time t), attesting to a pseudo-first-order reaction for the Pd^{II} complex $\mathbf{1}_{CN,Br}$. The slope of the straight line provided the value of the observed rate constant k_{obs}: $\ln x = -k_{obs}t$. A series of similar kinetic studies was performed by varying α and β, that is, the amounts of base and arylboronic acid $\mathbf{2}_H$ relative to the Pd^{II} complex **1**. Whatever the conditions, the ratio α/β was always maintained lower than unity because an excess of free OH^- ions made monitoring the increase in the oxidation current of $[Pd^0(PPh_3)_3]$ impossible due to a parasitic oxidation current (oxidation of free OH^-). $[Pd^0(PPh_3)_3]$ and ArAr′ were generated in similar yields and the reactions were almost quantitative (Table 1). In all investigated cases, the increase in the oxidation current of $[Pd^0(PPh_3)_3]$ (i.e., its concentration) with time was monotonous; no S-shaped curves were obtained. Moreover, the rate of formation of $[Pd^0(PPh_3)_3]$ was found to be sensitive to the concentration of $\mathbf{2}_H$. Consequently, if an intermediate complex was formed (such as $[ArPdAr'L_2]$), it immediately afforded $[Pd^0(PPh_3)_3]$. In other words, the rate observed in all experiments was that of the rate-determining transmetalation, the reductive elimination leading to $[Pd^0(PPh_3)_3]$ and ArAr′ always being faster under our experimental conditions. The variation of k_{obs} versus α and β was then investigated (Figure 2).

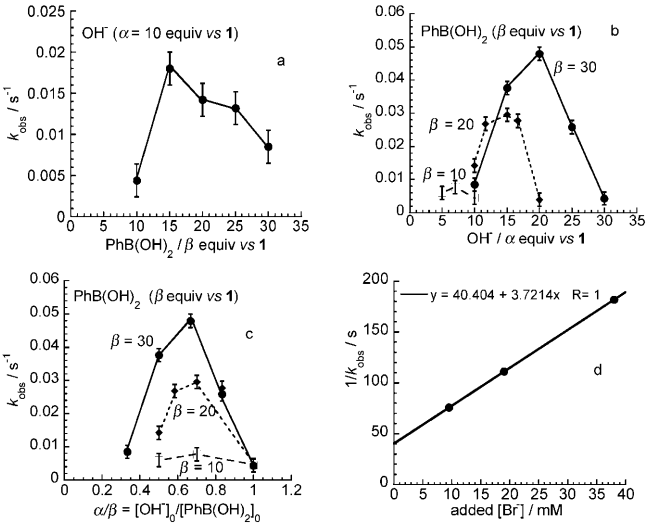

Figure 2. Reactions performed in DMF at 25 °C. Variation of the pseudo-first-order rate constant with α and β for the reaction of $PhB(OH)_2$ (β equiv) with $[(p\text{-NC-}C_6H_4)PdBr(PPh_3)_2]$ (**1**; $C_0 = 1.9$ mM) in the presence of PPh_3 (2 equiv) and OH^- (α equiv): a) Plot of k_{obs} versus β for $\alpha = 10$. b) Plots of k_{obs} versus α for $\beta = 10$, 20, and 30. c) Plot of k_{obs} versus α/β. d) Influence of the bromide concentration on the kinetics of the reaction of $[(p\text{-NC-}C_6H_4)PdBr(PPh_3)_2]$ ($C_0 = 1.9$ mM) with $PhB(OH)_2$ (20 equiv) in the presence of PPh_3 (2 equiv) and OH^- (15 equiv). Plot of $1/k_{obs}$ versus bromide concentration (introduced as $n\text{Bu}_4\text{NBr}$).

On the one hand, it was observed that for a constant amount of OH^- ($\alpha = 10$), k_{obs} increased with the concentration of $PhB(OH)_2$ and then decreased when the ratio β/α became higher than 1.5 (Figure 2a), leading to a bell-shaped curve. This suggested that at high $PhB(OH)_2$ concentrations, most OH^- ions were quenched to generate less reactive species. On the other hand, plots of k_{obs} versus OH^- concentration for different constant $PhB(OH)_2$ concentrations were all bell-shaped (Figure 2b), suggesting that the rate of the overall reaction strongly depended on the ratio α/β, as also illustrated in Figure 2c. The reactions became very slow when the amount of OH^- with respect to the $ArB(OH)_2$ was made too low or the ratio was close to unity.

The reactivity of [(*p*-NC-C_6H_4)PdBr(PPh_3)$_2$] (**1**$_{CN,Br}$; C_0 = 1.9 mM) with $PhB(OH)_2$ ($\beta = 20$) in the presence of OH^- ($\alpha = 15$) and PPh_3 (2 equiv) was also investigated in the presence of increasing amounts of bromide ions to explore the kinetics under the conditions of a real catalytic cycle having converted a significant fraction of ArBr. The higher the bromide concentration, the slower the reaction. The reaction order for Br^- was determined by plotting $1/k_{obs}$ versus bromide concentration (Figure 2d). A straight line was obtained with a positive intercept: $1/k_{obs} = a + b[Br^-]$. This positive intercept (40 s) was close to the value of $1/k_{obs}$ determined in the absence of added bromide (34 s; Figure 2b). The decelerating effect of bromide suggested that **1**$_{CN,Br}$ was in equilibrium with a more reactive species.

To identify the reactive species and to delineate the role of OH^-, which was evidenced to exert an accelerating or decelerating effect on the overall reaction (vide supra), the reactions of OH^- with all organic or organometallic species involved in the reaction were investigated.

Triple role of OH^- in the reaction of *trans*-[ArPdX(PPh_3)$_2$] with Ar′B(OH)$_2$: A first expected role of OH^- that was investigated was related to the known equilibrated formation of anionic $Ar'B(OH)_3^-$ in Scheme 7a.[14] To our knowledge,

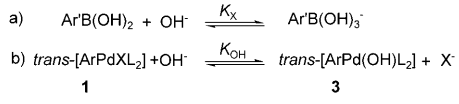

Scheme 7.

the equilibrium constant K_{OH} is not known in DMF. The equilibrium in the equation given in Scheme 7a was observed by ^{11}B NMR spectroscopy performed in DMF containing 10% [D_7]DMF at 20 °C. The integral of the sharp singlet of $PhB(OH)_3^-$ at $\delta = 5.18$ ppm[14b] increased at the expense of the integral of the broad singlet of $PhB(OH)_2$ at $\delta = 28.24$ ppm after successive additions of nBu$_4$NOH (1 M in MeOH) from 0.25 to 2 equivalents to $PhB(OH)_2$ (0.26 M). Note that the broad signal of $PhB(OH)_2$ could only be observed when the added base was substoichiometric, but in these cases the OH^- concentration was negligible and unknown. Consequently, K_{OH} could not be determined through such ^{11}B NMR experiments though they evidenced that the equilibrium constant has a value of at least a few thousands. The same conclusion was reached for *p*-MeO-C_6H_4-$B(OH)_2$ (br s, 29.43 ppm) leading to *p*-MeO-C_6H_4-$B(OH)_3^-$ (s, 5.26 ppm),[14b] showing K_{OH} to be too high to be determined by ^{11}B NMR spectroscopy under realistic conditions in DMF. Note that these results are perfectly consistent with those of the kinetic studies (vide infra), which indicates that $K_{OH}/K_X > 4 \times 10^3$ M^{-1} (Ar′ = Ph, vide infra for K_X). In neither case was an additional signal observed, even when an excess of nBu$_4$NOH was added, indicating that deprotonation of $Ar'B(OH)_2$ did not occur under our experimental conditions. Only aryl borates nBu$_4$NB(Ar′)$(OH)_3$ were generated, in agreement with the findings of Cammidge et al.[14b]

Consequently, in the presence of the base, two boron derivatives, the neutral $Ar'B(OH)_2$ and the ate species $Ar'B(OH)_3^-$, were present and might have been reactive in the transmetalation step.

A second role of OH^- that is generally invoked concerns the reversible exchange of the halide X in *trans*-[ArPdX(PPh_3)$_2$] (**1**) to generate *trans*-[ArPd(OH)(PPh_3)$_2$] (**3**) in Scheme 7b. In previous work, the formation of *trans*-[(Ph)Pd(OH)(PPh_3)$_2$] (^{31}P NMR, $\delta = 23.30$ ppm versus H_3PO_4) was observed when nBu$_4$NOH was added to *trans*-[(Ph)PdI(PPh_3)$_2$] ($\delta = 24.44$ ppm) in DMF containing 10% [D_6]acetone.[6b] Similarly, *trans*-[(Ph)Pd(OH)(PPh_3)$_2$] ($\delta = 23.98$ ppm) was formed when nBu$_4$NOH was added to *trans*-[(Ph)PdBr(PPh_3)$_2$] ($\delta = 23.80$ ppm) in $CDCl_3$[9a] or when aqueous NaOH was added to *trans*-[(Ph)PdBr(PPh_3)$_2$] in THF.[4b] Since all kinetic studies have been performed in the presence of PPh_3 (2 equiv), the reaction of *trans*-[(*p*-Z-C_6H_4)PdX(PPh_3)$_2$] (**1**$_{Z,X}$) with OH^- was also investigated in the presence of two equivalents of PPh_3 and monitored by ^{31}P NMR spectroscopy in $CDCl_3$, CD_2Cl_2, and DMF containing 7% [D_7]DMF (Table 2). The singlet due to **1**$_{CN,Br}$ progressively disappeared with the addition of OH^- (α equiv) to give a new singlet, the amplitude of which increased with α (Table 2). The same singlet was observed when OH^- was added to **1**$_{CN,I}$ or **1**$_{CN,Cl}$ (Table 2). This common singlet was thus assigned to *trans*-[(*p*-NC-C_6H_4)Pd(OH)(PPh_3)$_2$] (**3**$_{CN,OH}$) formed by X/OH exchange (Scheme 7b). The coexistence of sharp singlets for both *trans*-[(*p*-Z-C_6H_4)PdX(PPh_3)$_2$] (**1**$_{Z,X}$) and *trans*-[(*p*-Z-C_6H_4)Pd(OH)(PPh_3)$_2$] (**3**$_{Z,OH}$) for all investigated complexes (Z = CN, F, H; Table 2) and solvents indicated that the equilibrium in Scheme 7b was dynamically slow compared to the NMR timescale, but was nevertheless faster than the transmetalation step under the conditions of the reaction in Scheme 3 (vide infra). The equilibrium constant for the equation in Scheme 7b was determined in

Table 2. ^{31}P NMR shifts δ (101 MHz, H_3PO_4) at 22 °C.

trans-[Ar-PdX(PPh_3)$_2$] (**1**)	*trans*-[Ar-Pd(OH)(PPh_3)$_2$] (**3**)	δ [ppm]		
		CD_2Cl_2	$CDCl_3$	DMF
[(Ph)PdBrL$_2$]		23.78	23.80	24.06
	[(Ph)Pd(OH)L$_2$]	23.02[a]	23.98	22.42
[(*p*-NC-C_6H_4)PdClL$_2$]		24.20	23.85	
[(*p*-NC-C_6H_4)PdBrL$_2$]		23.88	23.79	23.91
[(*p*-NC-C_6H_4)PdIL$_2$]		22.81	22.85	
	[(*p*-NC-C_6H_4)Pd(OH)L$_2$]	23.23	23.98	22.40
[(*p*-F-C_6H_4)PdBrL$_2$]		23.83		24.13
	[(*p*-F-C_6H_4)Pd(OH)L$_2$]	23.10		22.47

[a] 23.3 ppm at 18 °C.[16]

DMF on the basis of ^{31}P NMR data: $K_X = 5 \pm 2$ (DMF, 22 °C) for the equilibrium $\mathbf{1}_{CN,Br}/\mathbf{3}_{CN,OH}$. Three equivalents of OH^- were required to fully displace the equilibrium towards $\mathbf{3}_{CN,OH}$ according to the NMR analysis.

The exchange of the bromide ligand in $\mathbf{1}_{CN,Br}$ by OH^- was also observed by cyclic voltammetry. The reduction peak of $\mathbf{1}_{CN,Br}$ (1.9 mM) in DMF at −1.83 V disappeared after the addition of three equivalents of OH^-. It was replaced by a new reduction peak located at a more negative potential (−2.00 V), characteristic of $\mathbf{3}_{CN,OH}$.

Therefore, the base OH^- was involved in two competitive equilibria (Scheme 7). This competition was controlled by the relative values of K_X and K_{OH} at a constant $Ar'B(OH)_2/[ArPdXL_2]$ ratio and by the ratio $Ar'B(OH)_2/[ArPdXL_2]$ at a given OH^- concentration. *trans*-$[ArPd(OH)(PPh_3)_2]$ appeared to be a likely intermediate in reactions with $Ar'B(OH)_2$ and/or $Ar'B(OH)_3^-$. Since *trans*-$[ArPd(OH)(PPh_3)_2]$ was in equilibrium with *trans*-$[ArPdX(PPh_3)_2]$ (Scheme 7b), its intrinsic reactivity could not be observed when starting from the latter. Consequently, *trans*-$[(Ph)Pd(OH)(PPh_3)_2]$ ($\mathbf{3}_{H,OH}$) was generated in situ in DMF by reacting PPh_3 (5.7 mM) with the *cis*+*trans* dimeric[15] $[\{(Ph)Pd(\mu\text{-}OH)(PPh_3)\}_2]$ ($C'_0 = 0.95$ mM; Scheme 8).[16] These concentrations were selected so that $PPh_3/Pd = 4$, that is to say, a ratio identical to that used in the kinetic experiments performed starting from *trans*-$[ArPdX(PPh_3)_2]$ (vide supra) and in the catalytic reactions.[1–3]

Scheme 8.

The intrinsic reactivity of *trans*-$[(Ph)Pd(OH)(PPh_3)_2]$ ($\mathbf{3}_{H,OH}$) with $Ar'B(OH)_2$ was then followed by cyclic voltammetry as detailed above for *trans*-$[ArPdX(PPh_3)_2]$, but in the absence of added OH^- (Scheme 9).

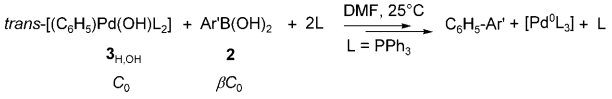

Scheme 9.

The dimer $[\{(Ph)Pd(\mu\text{-}OH)(PPh_3)\}_2]$ ($C'_0 = 0.95$ mM in DMF) exhibited an irreversible broad reduction peak (mixture of *cis* and *trans* isomers)[15] at around −2.10 V (Figure 3a). After the addition of PPh_3 (5.7 mM), the reduction peak became better defined and located at −2.15 V, attesting to the formation of *trans*-$[(Ph)Pd(OH)(PPh_3)_2]$ (Figure 3b).

Upon addition of $PhB(OH)_2$ (10 equiv/Pd), no $[Pd^0(PPh_3)_3]$ was formed since its oxidation peak was not observed when a cyclic voltammogram was obtained by first scanning towards oxidation potentials (from −0.5 to +0.6 V; Figure 3c). However, the reduction peak of *trans*-$[(Ph)Pd(OH)(PPh_3)_2]$ was no longer observed and a new reduction peak developed at a less negative potential (−1.62 V; Figure 3c). This intermediate species contained a Pd^{II} center, since its electrochemical reduction led to $[Pd^0(PPh_3)_3]$, as evidenced by the detection of its oxidation peak during the reverse scan. The intermediate structure was thus assigned to the mixed complex *trans*-$[(Ph)Pd(Ph)(PPh_3)_2]$. This intermediate was stable during at least 50 min. In a previous study concerning the mechanism of the $[Pd^0(PPh_3)_4]$-catalyzed homocoupling of arylboronic acids under dioxygen, we also provided evidence for the formation of stable intermediate *trans*-bis(aryl)palladium(II) complexes in $CDCl_3$,[9a] for example: 1) *trans*-$[(p\text{-}NC\text{-}C_6H_4)Pd(Ph)(PPh_3)_2]$ formed upon addition of $p\text{-}NC\text{-}C_6H_4\text{-}B(OH)_2$ (1.5 equiv) to *trans*-$[(Ph)Pd(OH)(PPh_3)_2]$ and 2) *trans*-$[(p\text{-}MeO\text{-}C_6H_4)Pd(C_6H_4\text{-}p\text{-}CN)(PPh_3)_2]$ formed upon addition of $p\text{-}NC\text{-}C_6H_4\text{-}B(OH)_2$ (1.5 equiv) to *trans*-$[(p\text{-}MeO\text{-}C_6H_4)Pd(OH)(PPh_3)_2]$. These complexes generated in situ in $CDCl_3$ were fully characterized by ^{31}P NMR and ^1H NMR spectroscopy (see Table 6 and Figure 3 in reference [9a]). This and the present voltammetric observations suggest that $Ar'B(OH)_2$ reacts with *trans*-$[ArPd(OH)(PPh_3)_2]$ in a transmetalation step to generate quite stable intermediates *trans*-$[ArPdAr'(PPh_3)_2]$.[17] However, this raised the question as to why such intermediate complexes were not observed in the reaction of *trans*-$[(p\text{-}NC\text{-}C_6H_4)PdBr(PPh_3)_2]$ with $PhB(OH)_2$ performed in the presence of OH^- as base (vide supra). There-

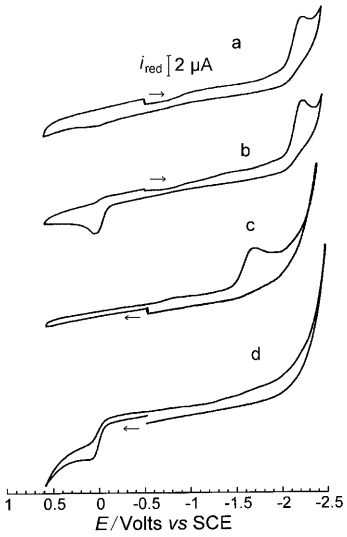

Figure 3. Cyclic voltammetry performed at a fixed gold disk electrode ($d = 1$ mm) in DMF containing 0.3 M nBu_4NBF_4 at a scan rate of 0.5 $V s^{-1}$ at 25 °C. a) Reduction of $[\{(Ph)Pd(\mu\text{-}OH)(PPh_3)\}_2]$ (0.95 mM). b) Reduction of *trans*-$[(Ph)Pd(OH)(PPh_3)_2]$ (1.9 mM) generated by reaction of PPh_3 (5.7 mM) with $[\{(Ph)Pd(\mu\text{-}OH)(PPh_3)\}_2]$ (0.95 mM). c) Reduction of *trans*-$[(Ph)Pd(Ph)(PPh_3)_2]$ formed by addition of $PhB(OH)_2$ (19 mM) to *trans*-$[(Ph)Pd(OH)(PPh_3)_2]$ generated as in b). d) Oxidation of $[Pd^0(PPh_3)_3]$ formed after addition of OH^- (9.5 mM) to *trans*-$[(Ph)Pd(Ph)(PPh_3)_2]$ generated as in c).

fore, OH^- (5 equiv/Pd) was added to the intermediate *trans*-[(Ph)Pd(Ph)(PPh_3)$_2$], 50 min after its formation. Gratifyingly, its reduction peak rapidly disappeared (within 1 min), while the solution turned yellow. [$Pd^0(PPh_3)_3$] was formed, as revealed by its oxidation peak at +0.08 V, when a voltammogram was obtained by first scanning towards oxidation potentials (from −0.5 to +0.6 V; Figure 3d).[18]

Therefore, a third unexpected role of OH^- emerged: promotion of reductive elimination from stable *trans*-bis(aryl)palladium complexes, presumably through the addition of OH^- as a fifth ligand[19,20] (path A in Scheme 10) and circumvention of the thermodynamically uphill formation of a *cis* complex (path B in Scheme 10).

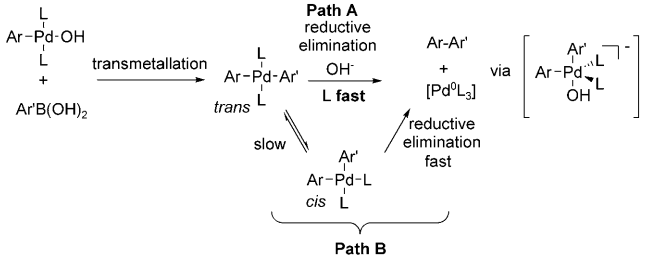

Scheme 10.

In another series of experiments, *p*-MeO-C_6H_4-$B(OH)_2$ (1.5 equiv) was added to *trans*-[(Ph)Pd(OH)(PPh_3)$_2$] (1.9 mM). The reduction peak of this complex slowly disappeared with time and coexisted with a new reduction peak at a less negative potential (−1.64 V), which was assigned to *trans*-[(*p*-MeO-C_6H_4)Pd(Ph)(PPh_3)$_2$]. After 15 min, the oxidation peak of [$Pd^0(PPh_3)_2$] was detected at +0.06 V. This peak was fully developed after 2 h and the reversible reduction peak of the coupling product *p*-MeO-C_6H_4-Ph was observed at −2.50 V. In a previous study, we observed that *p*-MeO-C_6H_4-Ph was eventually formed upon reacting $PhB(OH)_2$ (1.5 equiv) with [(*p*-MeO-C_6H_4)Pd(OH)(PPh_3)$_2$].[9a] Consequently, the intermediate complex *trans*-[(*p*-MeO-C_6H_4)Pd(Ph)(PPh_3)$_2$] slowly underwent reductive elimination after isomerization to the *cis* complex (path B in Scheme 10) with a half-reaction time, $t_{1/2}$, estimated to be of the order of 10 min. The disfavored *trans*–*cis* isomerization equilibrium was then continuously displaced as a result of the fast reductive elimination being favored by the electron-donating OMe substituent (path B). However, this process was too slow to account for the fast overall reactions in the presence of hydroxide.[21a] The question then arose as to whether hydroxide OH^- would favor the reductive elimination from *trans*-[(*p*-MeO-C_6H_4)Pd(Ph)(PPh_3)$_2$] through path A in Scheme 10, as observed for *trans*-[(Ph)Pd(Ph)(PPh_3)$_2$] (vide supra). The accelerating effect of OH^- was confirmed by adding it to a solution of transient *trans*-[(*p*-MeO-C_6H_4)Pd(Ph)(PPh_3)$_2$] formed by reacting *trans*-[(Ph)Pd(OH)(PPh_3)$_2$] (1.9 mM) with *p*-MeO-C_6H_4-$B(OH)_2$ (5 equiv). Whereas [$Pd^0(PPh_3)_3$] was formed in 23% yield after 5 min in the absence of OH^-, the introduction of OH^- (3.4 equiv) resulted in the complete consumption of *trans*-[(*p*-MeO-C_6H_4)Pd(Ph)(PPh_3)$_2$] within 2 min and the quantitative formation of [$Pd^0(PPh_3)_3$], as revealed by the corresponding voltammogram.[21]

Therefore, the reductive elimination from *trans*-[(*p*-MeO-C_6H_4)Pd(Ph)(PPh_3)$_2$] was also accelerated by the base OH^- and proceeded through path A in Scheme 10, this being faster than the overall step B and than the transmetalation. As such, the transmetalation became the rate-determining step in the presence of OH^-, whatever the substituent on the Ar or Ar′ groups.

Mechanism of the reaction of *trans*-[ArPdX(PPh_3)$_2$] with Ar′B(OH)$_2$ in the presence of the base OH^-: From the above experiments, it emerged that *trans*-[ArPdBr(PPh_3)$_2$] does not react with Ar′$B(OH)_2$ (no reaction in the absence of OH^-). This rules out route a in Scheme 11. However,

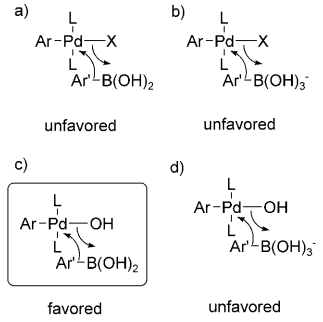

Scheme 11. Pathways for the transmetalation step.

trans-[ArPd(OH)(PPh_3)$_2$] reacts with Ar′$B(OH)_2$ as a consequence of the high oxophilicity of the boron (route c in Scheme 11), which is also supported by DFT calculations (with PH_3 as ligand).[7a] As mentioned in the introduction, such a pathway through a four-centered transition state was proposed by Soderquist et al. for an alkylborane.[4b] The reactivity of Rh–OH bonds with arylboronic acids has also been established by the groups of Hayashi and Hartwig.[22]

From Figure 2, it is evident that too large an excess of OH^- with respect to the [ArPdXL_2] complex inhibits the reaction, which indicates that Ar′$B(OH)_3^-$ does not react with [ArPd(OH)L_2] (route d in Scheme 11), at least not at a sufficient rate. In another experiment, we indeed observed that no reaction took place when *p*-NC-C_6H_4-$B(OH)_3^-$ (generated by reacting *p*-NC-C_6H_4-$B(OH)_2$ with 5 equiv of OH^-) was added to [(Ph)Pd(OH)(PPh_3)$_2$]. Route d was thus definitively ruled out. Ar′$B(OH)_3^-$ is considerably less reactive than Ar′$B(OH)_2$ towards *trans*-[ArPd(OH)(PPh_3)$_2$], presumably because of a difficult transfer of an OH group to a negatively charged species.

Route b in Scheme 11 might be an alternative and so needed to be examined.[4,7a,b] To test such a pathway, we had to investigate the reaction of $PhB(OH)_3^-$ with [(*p*-NC-C_6H_4)PdBr(PPh_3)$_2$] in the presence of a large excess of bromide ions so that the equilibrium in Scheme 7b was fully

displaced towards [(*p*-NC-C_6H_4)PdBr(PPh_3)$_2$]. The reaction of $PhB(OH)_3^-$ (generated by addition of excess OH^- (30 equiv) to $PhB(OH)_2$ (20 equiv)) with [(*p*-NC-C_6H_4)PdBr(PPh_3)$_2$] ($C_0 = 2.5$ mM) in the presence of PPh_3 (2 equiv) and a large amount of bromide ions (100 equiv) was monitored by cyclic voltammetry. [(*p*-NC-C_6H_4)PdBr(PPh_3)$_2$] was detected by its reduction peak in a voltammogram obtained by scanning towards reduction potentials, but not [(*p*-NC-C_6H_4)Pd(OH)(PPh_3)$_2$], indicating that the excess of bromide ions had been judiciously selected to counterbalance the effect of the hydroxide (in excess relative to $PhB(OH)_2$). No reaction between [(*p*-NC-C_6H_4)PdBr(PPh_3)$_2$] and $PhB(OH)_3^-$ took place, even after 3 h. The cross-coupling product was not observed. This experiment rules out path b in Scheme 11.

The inhibiting effect of bromide ions observed in Figure 2d also supported route c. Indeed, the higher the bromide ion concentration, the lower the [$ArPd(OH)L_2$] concentration (due to a shift in the equilibrium in Scheme 7b to its left-hand side), and hence the slower the reaction. This also confirms that route b is definitively less favored.

Based on all these data, the mechanism of the transmetalation/reductive elimination may be kinetically depicted as in Scheme 12.

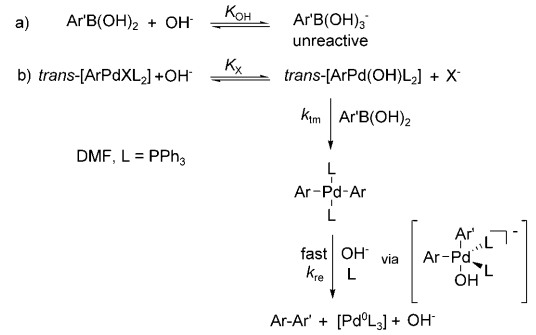

Scheme 12. Mechanism for the transmetalation/reductive elimination.

The base OH^- is required to generate the reactive *trans*-[$ArPd(OH)(PPh_3)_2$], which reacts with $Ar'B(OH)_2$. This is consistent with the higher oxophilicity[22] of the boron atom compared to its halogenophilicity (the latter was evidenced by Brown et al.[23]). OH^- is also required to induce the reductive elimination from *trans*-[$ArPdAr'(PPh_3)_2$]. This reaction, which is presumably catalytic in OH^-, becomes so fast in the presence of the base that the transmetalation becomes the rate-determining step in Scheme 12. When the concentration of OH^- is increased, the equilibrium in Equation (b) in Scheme 12 is shifted towards the reactive *trans*-[$ArPd(OH)L_2$], but this also shifts the equilibrium in Scheme 12a towards the comparatively unreactive $Ar'B(OH)_3^-$. As a consequence of OH^- ions being involved in two opposing reactions, the rate of the transmetalation (reflected by the magnitude of k_{obs}) conforms to a bell-shaped curve as the OH^- concentration is increased (Figure 2b, Figure 4).

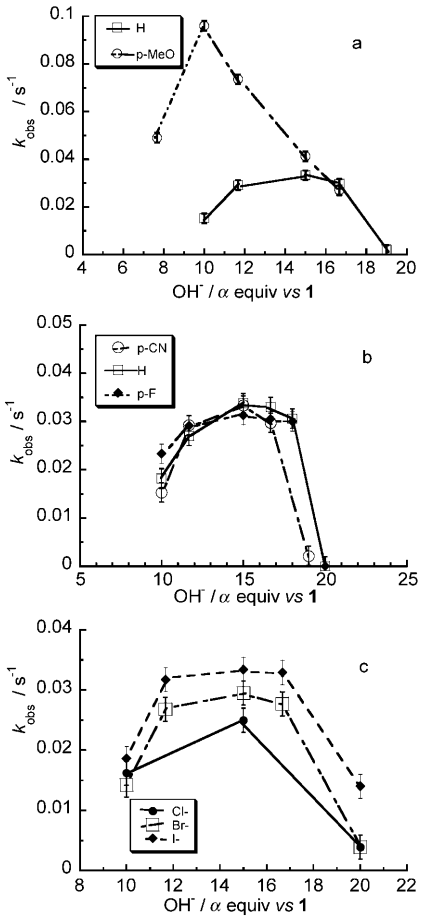

Figure 4. Reactions performed in DMF at 25 °C. a) Influence of the substituent Z′ of *p*-Z′-C_6H_4-$B(OH)_2$ (20 equiv) on the rate of its reaction with [(*p*-NC-C_6H_4)PdBr(PPh_3)$_2$] (**1**; $C_0 = 1.9$ mM) in the presence of PPh_3 (2 equiv) and OH^- (α equiv). Plot of k_{obs} versus α. b) Influence of the substituent Z of [(*p*-Z-C_6H_4)PdBr(PPh_3)$_2$] (**1**; $C_0 = 1.9$ mM) on the rate of its reaction with $PhB(OH)_2$ (20 equiv) in the presence of PPh_3 (2 equiv) and OH^- (α equiv). Plot of k_{obs} versus α. c) Influence of the halide X of [(*p*-NC-C_6H_4)PdX(PPh_3)$_2$] (**1**; $C_0 = 1.9$ mM) on the rate of its reaction with $PhB(OH)_2$ (20 equiv) in the presence of PPh_3 (2 equiv) and OH^- (α equiv). Plot of k_{obs} versus α.

Finally, the effect of the substituent Z′ of *p*-Z′-C_6H_4-$B(OH)_2$ (**2**$_{Z'}$; Z′ = CN,[24] H, MeO; 20 equiv) in the reaction with [(*p*-NC-C_6H_4)PdBrL_2] (**1**$_{CN,Br}$) has been investigated as a function of the initial OH^- concentration. The variation of k_{obs} always conformed to a bell-shaped curve (Figure 4a). Whatever the amount of OH^-, the same reactivity order was observed: MeO ⩾ H. $Ar'B(OH)_2$ was indeed more reactive (route c in Scheme 11) because it is more nucleophilic when Ar′ is substituted by an electron-donor group.

The effect of the substituent Z in [(*p*-Z-C_6H_4)PdBr(PPh_3)$_2$] (**1**$_{Z,Br}$; Z = CN, F, H)[25] in the reaction with $PhB(OH)_2$ (20 equiv) has been investigated as a function of the initial OH^- concentration (Figure 4b, Table 1). Again, the variation of k_{obs} always conformed to a bell-shaped curve. At identical initial concentrations of OH^-, the reactivities of **1**$_{Z,Br}$ were seen to be quite similar or did not vary significantly with Z (Figure 4b). The rate-determining trans-

metalation concerns the Pd–OH bond. The latter must not be too strongly affected by the electronic properties of the Ar group attached to the Pd^{II} center in *trans*-[ArPd(OH)-$(PPh_3)_2$] (weak *trans* effect). The same must apply for the substitution of Br^- by OH^- in *trans*-[ArPdBr$(PPh_3)_2$].

The effect of the halide X borne by [(*p*-NC-C_6H_4)PdX-$(PPh_3)_2$] ($\mathbf{1}_{CN,X}$; X = I, Br, Cl) in its reaction with $PhB(OH)_2$ (20 equiv) has been investigated as a function of the initial OH^- concentration (Figure 4c, Table 1). Again, the variation of k_{obs} always conformed to a bell-shaped curve. At identical initial OH^- concentrations, the reactivity order was found to be: $[ArPdIL_2] > [ArPdBrL_2] > [ArPdClL_2]$. Only the Pd–X bond is affected by the substitution of X^- by OH^-. This suggests that the amount of the reactive [ArPd(OH)$(PPh_3)_2$] species increased on going from Cl to I, and consequently that $K_I > K_{Br} > K_{Cl}$ in DMF.[26]

Kinetic law: A general kinetic law was derived based on the formulation in Scheme 12, assuming that the reductive elimination was fast enough for the rate-determining step to be the transmetalation (rate constant k_{tm}). Then, rate $= d[Pd^0]/dt = -d[Pd^{II}]/dt$, where the overall rate of the reaction formulated in Equation (1) introduced an apparent rate "constant" (see below), k_{obs}, the expression for which is given by Equation (2):[27a] ,

$$\text{rate} = k_{obs}[Pd^{II}]_{total} \quad (1)$$

$$k_{obs} = k_{tm}\beta C_0 \frac{1}{1 + K_{OH}[OH^-]} \frac{K_x[OH^-]}{[X^-] + K_x[OH^-]} \quad (2)$$

Equation (2) shows that although the expression for k_{obs} is valid at any instant during the reaction course, this term may not be considered as a pseudo-first-order rate constant in an absolute view because $[X^-]$ and $[OH^-]$ are susceptible to variations during the reaction course when the respective species are not in excess. This is particularly the case for $[X^-]$, since this term varies from near zero at initial time to C_0 at completion of the reaction. Variations in $[OH^-]$ are expected to be less severe during the reaction course as soon as α and β, as well as $(\beta-\alpha)$, are much larger than unity.[27b] Indeed, when these conditions are fulfilled, OH^- is in excess so that its concentration may safely be considered as a constant during the reaction course.[28]

Kinetic consequences in the absence of an excess of X^-: Under such conditions, $[X^-]$ (and hence $[OH^-]$) is expected to vary during the reaction course. In these circumstances, one generally relies on the so-called "initial rate" method, which amounts to considering the initial slope of the temporal variation of $\ln x$, since the initial concentrations of all reagents are known. However, in the present circumstances, this method is not applicable because: 1) the need for rapid mixing at initial times precludes any reliable amperometric measurements of initial rates, and 2) the initial $[X^-]$ would not be known independently. For this reason, we relied on the measurement of $k_{obs(50\%)}$, which is given by the slope of the variation of $\ln x$ versus time measured at 50% conversion, at which, by definition, $[X^-]$ was close to $C_0/2$. The expression for $k_{obs(50\%)}$ is then given by Equation (3):

$$k_{obs(50\%)} = k_{tm}\beta C_0 \frac{1}{1 + K_{OH}[OH^-]} \frac{K_x[OH^-]}{C_0/2 + K_x[OH^-]} \quad (3)$$

If $[OH^-] \ll 1/K_{OH}$ and $[OH^-] \ll C_0/(2K_X)$, then $k_{obs(50\%)} \rightarrow 2k_{tm}\beta K_X[OH^-]$, so that $k_{obs(50\%)}$ increases with $[OH^-]$. Conversely, if $[OH^-] \gg 1/K_{OH}$ and $[OH^-] \gg C_0/(2K_X)$, $k_{obs(50\%)} \rightarrow k_{tm}\beta C_0/(K_{OH}[OH^-])$, which shows that the reaction rate decreases upon increasing $[OH^-]$. Since for any given β value ($\beta \gg 1$) and provided that $(\beta-\alpha) \gg 1$, $[OH^-]$ is mostly dictated by the equilibrium in Scheme 12a, that is to say, by the value of α/β (see below). This indicates that $k_{obs(50\%)}$ passes through a maximum when α/β is varied from zero to unity, in agreement with the experimental observations (compare Figure 2b,c). Conversely, when $[OH^-] \ll 1/K_{OH}$ or $[OH^-] \ll C_0/(2K_X)$, a maximum is also predicted, as observed in Figure 2b,c. The maximum of $k_{obs(50\%)}$ is achieved when the derivative of its formulation versus $[OH^-]$ in Equation (3) is zero, that is, when $[OH^-]_{max} = [C_0/(2K_XK_{OH})]^{1/2}$.[27a,29]

By application of the conservation of matter laws for $[OH^-]$ and $[X^-]$ and taking into account the expressions of the two mass action laws relative to the equilibria in Scheme 12, it can easily be shown that this condition means that the maximum of $k_{obs(50\%)}$ can be given by Equation (4) in which $\Gamma = [C_0K_{OH}/(2K_X)]^{1/2}$.

$$(\alpha/\beta)_{max} = \Gamma/(\beta C_0 K_{OH}) + \Gamma/(1+\Gamma) \quad (4)$$

This expression shows that as soon as β is extremely large (as it is, for example, under the conditions of Figure 2b,c), the value of the ratio $(\alpha/\beta)_{max}$ at which the maximum of $k_{obs(50\%)}$ is observed is almost independent of β, as has been borne out experimentally (compare Figure 2b,c): $(\alpha/\beta)_{max} \approx \Gamma/(1+\Gamma)$. Experimentally, one observes that $(\alpha/\beta)_{max} \approx 2/3$, which indicates that $\Gamma \approx 2$. Since $C_0 \approx 2\times10^{-3}$ M, $K_{OH}/K_X \approx 4\times10^3\ M^{-1}$.[30]

Therefore, as evidenced by the kinetic law in Equation (2), the base OH^- plays two roles, the antagonistic influences of which first favor (low OH^- concentrations) and then disfavor (high OH^- concentrations) the rate of the overall catalytic sequence, as observed experimentally (Figures 2a–c and 4).[31]

Consequences for the reaction rate in the presence of an excess of X^-: When α, β, and $(\beta-\alpha)$ are all larger than unity and $[X^-] \gg C_0$, the expression for k_{obs} in Equation (2) shows that this term is constant during the whole reaction course, that is, that it acts as a fully fledged pseudo-rate constant and perfect exponential conversions are observed. At high halide concentrations, the equilibrium in Scheme 12b is completely shifted towards its left-hand side, so that the concentration of OH^- is controlled only by K_{OH}, α, and β. It is given by $[OH^-] = 1/\{K_{OH}[(\beta/\alpha)-1)]\}$ and is therefore constant during the reaction course as well as for any set of reactions performed at a constant α/β ratio. In addition, Equa-

tion (2) shows that $1/k_{obs}$ should vary linearly with the concentration of X^- according to Equation (5) in which μ and ν are constant for any given α/β ratio and C_0.

$$\frac{1}{k_{obs}} = \frac{1+K_{OH}[OH^-]}{k_{tm}\beta C_0} + \frac{1+K_{OH}[OH^-]}{k_{tm}\beta C_0 K_x[OH^-]}[X^-] = \mu + \nu[X^-] \quad (5)$$

This predicted hyperbolic decelerating effect of bromide is in full agreement with the experimental law observed in Figure 2d, confirming the mechanism presented in Scheme 12.

Therefore, although the kinetic law in Equations (1) and (2) is too complex to allow a complete quantitative kinetic characterization of the reaction mechanism under all experimental circumstances (that is to say, it could not be verified quantitatively when $[X^-] \ll C_0$ and at the same time $\beta-\alpha$ was not much larger than unity), all of its predictions were borne out, at least qualitatively. This particularly applies to the observation of a definite rate maximum imposed mostly by the value of the ratio α/β and a hyperbolic deceleration upon increasing $[X^-]$. This validates kinetically the main hypotheses derived from a series of experiments, that is to say, the fact that whenever the oxidative addition is fast enough, the rate-determining step of the overall catalytic cycle is the transmetalation, the effective rate of which is strongly influenced by the two equilibria in Scheme 12; note that the oxidative addition may become rate-determining when the aryl halide is not sufficiently reactive, as would occur for aryl chlorides and $L=PPh_3$, which would introduce another complexity that has not been taken into account within the framework of this work). Hence, it may be safely concluded that the mechanism of the Suzuki–Miyaura reaction can be depicted as in Scheme 13 when the base is OH^-.[32]

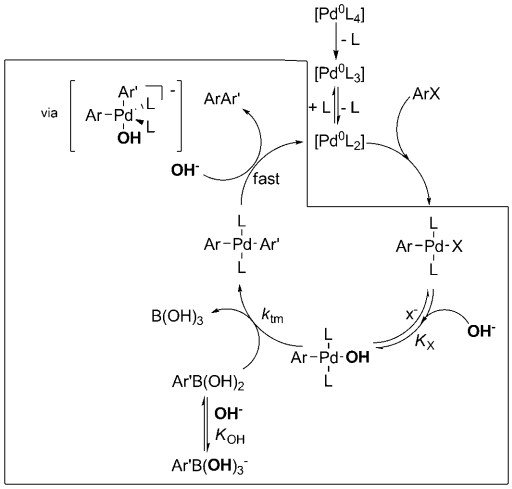

Scheme 13.

Conclusion

In studying the mechanism of the Suzuki–Miyaura reaction, OH^- has been shown to be crucial in promoting the transmetalation step and, unexpectedly, also serves to accelerate the reductive elimination step. However, upon increasing the OH^- concentration, the reaction slowed down drastically. In fact, the base OH^- plays three roles. Two are positive: 1) formation of $[ArPd(OH)(PPh_3)_2]$, which reacts with $Ar'B(OH)_2$, and 2) unexpected promotion of reductive elimination from the intermediate complex *trans*-$[ArPdAr'(PPh_3)_2]$. The negative contribution relates to the competitive formation of the poorly reactive $Ar'B(OH)_3^-$. These opposite effects are fully incorporated in the overall mechanism depicted in Scheme 13. As a consequence of these antagonistic effects, the overall reactivity is controlled by the initial concentration of OH^-, and passes through a maximum as the concentration of OH^- is increased. At a given concentration of $Ar'B(OH)_2$, a low concentration of OH^- results in a slow reaction because of a too low concentration of the reactive $[ArPd(OH)(PPh_3)_2]$. At high concentrations of OH^-, the reaction becomes slow because of the low concentration of the reactive $Ar'B(OH)_2$, the latter being mainly transformed to the unreactive $Ar'B(OH)_3^-$. In all investigated cases, the reaction of $[ArPd(OH)(PPh_3)_2]$ with $Ar'B(OH)_2$ (transmetalation) proved to be rate-determining. It was followed by a reductive elimination, which became faster in the presence of the base, presumably through a catalytic pathway involving a pentacoordinated anionic palladium complex (Scheme 13).

Consequently, in the optimization of Suzuki–Miyaura reactions, not only must the nature of the base be screened, as is usually performed, but the relative amount of the base must also be precisely controlled in each case. Indeed, the exact positions of the two equilibria that regulate the ratios $[ArPdXL_2]/[ArPd(base)L_2]$ and $ArB(OH)_2/Ar'B(OH)_2(base)^-$ are base-dependent. Hence, a high concentration of the base does not guarantee a fast reaction. The role of carbonate as another base is presently under investigation to offer a broader view of the conditions favoring this important reaction.

Experimental Section

General: ^{31}P NMR spectra were recorded on a Bruker spectrometer (101 MHz) with H_3PO_4 as an external reference. ^{11}B NMR spectra were recorded from solutions in $[D_7]$DMF on a Bruker spectrometer (128 MHz) with $Et_2O{\cdot}BF_3$ as an external reference (see the Supporting Information for a typical procedure).

Chemicals: DMF was distilled from calcium hydride under vacuum and kept under argon. PPh_3, $PhB(OH)_2$, 4-NC-C_6H_4-$B(OH)_2$, and 4-MeO-C_6H_4-$B(OH)_2$ were obtained from commercial sources and used as received. nBu$_4$NOH (1 M in MeOH) was also a commercial product. [(*p*-NC-C_6H_4)PdX$(PPh_3)_2$] (X = I, Br, Cl), [(*p*-Z-C_6H_4)PdBr$(PPh_3)_2$] ($\mathbf{1}_{Z,Br}$; Z = CN, F, H),[10] and the dimeric complex $[\{(Ph)Pd(\mu\text{-}OH)(PPh_3)\}_2]$[15] were synthesized according to literature procedures.

Typical procedure for reactions of $Ar'B(OH)_2$ with $[ArPdX(PPh_3)_2]$, as monitored by cyclic voltammetry: All experiments were performed

under argon atmosphere. Experiments were carried out in a thermostatted three-electrode cell connected to a Schlenk line. The counter electrode was a platinum wire of approximately 1 cm^2 apparent surface area; the reference was a saturated calomel electrode separated from the solution by a bridge filled with a 0.3 M solution of nBu_4NBF_4 in DMF (2 mL). A degassed 0.3 M solution of nBu_4NBF_4 in DMF (18 mL) was added to the cell, followed by *trans*-[(*p*-NC-C_6H_4)$PdBr(PPh_3)_2$] (30.7 mg, 0.037 mmol) to give a 1.9 mM solution. A cyclic voltammogram was first obtained by scanning towards reduction potentials at a fixed gold disk electrode ($d=0.5$ mm) at 25 °C at a scan rate of 0.5 $V s^{-1}$. PPh_3 (20 mg, 0.074 mmol) was then added and a further voltammogram was measured (Figure 1a). $PhB(OH)_2$ (90 mg, 0.74 mmol) was then added, and the subsequently obtained voltammogram was not modified. A 1 M solution of nBu_4NOH in MeOH (370 μL, 0.37 mmol) was then added, whereupon the solution turned yellow. A cyclic voltammogram was measured by scanning towards reduction potentials after 400 s (Figure 1b), which revealed the reversible reduction peak of *p*-NC-C_6H_4-Ph. Its yield (95%) was determined after the addition of an authentic sample of commercially available *p*-NC-C_6H_4-Ph (6.6 mg, 0.037 mmol). A cyclic voltammogram was then measured by first scanning towards oxidation potentials (Figure 1c), which revealed the reversible oxidation peak of $[Pd^0(PPh_3)_3]$. Its yield (94%) was determined after the addition of an authentic sample of $[Pd^0(PPh_3)_4]$ (21 mg, 0.0185 mmol).

Typical procedure for reactions of Ar'B(OH)$_2$ with [ArPd(OH)(PPh$_3$)$_2$], as monitored by cyclic voltammetry: *trans*-[(Ph)Pd(OH)$(PPh_3)_2$] was generated in situ in an electrochemical cell. For this, [{(Ph)Pd(μ-OH)(PPh_3)}$_2$] (10.5 mg, 0.0114 mmol) was added to an electrochemical cell containing a 0.3 M solution of nBu_4NBF_4 in DMF (12 mL) at 25 °C. A cyclic voltammogram was first measured towards reduction potentials at a fixed gold disk electrode ($d=1$ mm) at a scan rate of 0.5 $V s^{-1}$ (Figure 3a). Addition of PPh_3 (18 mg, 0.068 mmol) resulted in the formation of *trans*-[(Ph)Pd(OH)$(PPh_3)_2$], as observed by cyclic voltammetry first performed towards reduction potentials (Figure 3b). $PhB(OH)_2$ (27.6 mg, 0.23 mmol) was then added to the cell. The complex *trans*-[(Ph)Pd(Ph)-$(PPh_3)_2$] was formed, as revealed by a cyclic voltammogram obtained by first scanning towards reduction potentials (Figure 3c). This complex proved to be stable with time until the introduction of nBu_4NOH (114 μL, 0.114 mmol). The reduction peak of *trans*-[(Ph)Pd(Ph)$(PPh_3)_2$] was no longer detected and $[Pd^0(PPh_3)_3]$ was formed, as attested by its oxidation peak (Figure 3d).

Typical procedure for the kinetics of the reaction of *trans*-[ArPdX-(PPh$_3$)$_2$] with arylboronic acids, as monitored by chronoamperometry: All experiments were performed under argon atmosphere. Experiments were carried out in a three-electrode cell thermostatted at 25 °C and connected to a Schlenk line, as used above for cyclic voltammetry. The counter electrode was a platinum wire of about 1 cm^2 apparent surface area, and the reference was a saturated calomel electrode separated from the solution by a bridge filled with a 0.3 M solution of nBu_4NBF_4 in DMF (2 mL). A degassed 0.3 M solution of nBu_4NBF_4 in DMF (16 mL) was introduced into the cell, followed by [(*p*-NC-C_6H_4)$PdBr(PPh_3)_2$] (24 mg, 0.03 mmol, 1.9 mM), PPh_3 (16 mg, 0.06 mmol), and $PhB(OH)_2$ (73 mg, 0.6 mmol). Kinetic measurements were performed at a rotating gold disk electrode ($d=2$ mm, inserted into a Teflon holder, EDI 65109, Radiometer) with an angular velocity of 105 rad s^{-1} (Radiometer controvit) at 25 °C. The rotating electrode was polarized at +0.05 V on the oxidation wave of $[Pd^0(PPh_3)_3]$. A 1 M solution of nBu_4NOH in MeOH (300 μL, 0.3 mmol) was then added to the cell and the increase in the oxidation current of $[Pd^0(PPh_3)_3]$ was recorded versus time up to a constant limit value.

Acknowledgements

This work has been supported in part by the Centre National de la Recherche Scientifique (UMR CNRS-ENS-UPMC 8640) and the Ministère de la Recherche (Ecole Normale Supérieure). We thank Johnson Matthey for a generous loan of palladium salt. Marie-Noelle Rager is gratefully thanked for performing the ^{11}B NMR experiments.

[1] N. Miyaura, T. Yanagi, A. Suzuki, *Synth. Commun.* **1981**, *11*, 513–519.

[2] For reviews, see: a) A. Suzuki, *Pure Appl. Chem.* **1985**, *57*, 1749–1758; b) A. Suzuki, *Pure Appl. Chem.* **1991**, *63*, 419–422; c) N. Miyaura, A. Suzuki, *Chem. Rev.* **1995**, *95*, 2457–2483; d) N. Miyaura, in *Advances in Metal–Organic Chemistry, Vol. 6* (Ed.: L. S. Liebeskind), JAI Press, Greenwich, **1998**, pp. 187–243; e) A. Suzuki, *J. Organomet. Chem.* **1999**, *576*, 147–168; f) N. Miyaura, *J. Organomet. Chem.* **2002**, *653*, 54–57; g) F. Alonso, I. P. Beletskaya, M. Yus, *Tetrahedron* **2008**, *64*, 3047–3101.

[3] For a screening of bases, see: T. Watanabe, N. Miyaura, A. Suzuki, *Synlett* **1992**, 207–210.

[4] For mechanistic investigations, see: a) G. B. Smith, G. C. Dezeny, D. L. Hughes, A. O. King, T. R. Verhoeven, *J. Org. Chem.* **1994**, *59*, 8151–8156; b) K. Matos, J. A. Soderquist, *J. Org. Chem.* **1998**, *63*, 461–470.

[5] When vinyl- or allenyl-$[PdXL_2]$ (X = halide, L = PPh_3) is formed, a transmetalation of vinyl- or allenyl-$[Pd(OR)L_2]$ (RO^- used as a base; R = Me) with an aryl- or vinyl-boron derivative is proposed; a) N. Miyaura, K. Yamada, H. Suginome, A. Suzuki, *J. Am. Chem. Soc.* **1985**, *107*, 972–980; b) T. Moriya, N. Miyaura, A. Suzuki, *Synlett* **1994**, 149–151.

[6] For X/OAc exchange, see: a) C. Amatore, A. Jutand, M. A. M'Barki, *Organometallics* **1992**, *11*, 3009–3013; b) C. Amatore, E. Carré, A. Jutand, M. A. M'Barki, G. Meyer, *Organometallics* **1995**, *14*, 5605–5614.

[7] a) A. A. C. Braga, N. H. Morgon, G. Ujaque, A. Llédos, F. Maseras, *J. Organomet. Chem.* **2006**, *691*, 4459–4466; b) J. Jover, N. Fey, M. Purdie, G. C. Lloyd-Jones, J. N. Harvey, *J. Mol. Catal. A: Chem* **2010**, *324*, 39–47; for vinyl-$[PdX(PH_3)_2]$, see: c) A. A. C. Braga, N. H. Morgon, G. Ujaque, F. Maseras, *J. Am. Chem. Soc.* **2005**, *127*, 9298–9307; d) A. A. C. Braga, G. Ujaque, F. Maseras, *Organometallics* **2006**, *25*, 3647–3658.

[8] a) J.-F. Fauvarque, F. Pflüger, M. Troupel, *J. Organomet. Chem.* **1981**, *208*, 419–427; b) C. Amatore, F. Pflüger, *Organometallics* **1990**, *9*, 2276–2282.

[9] a) C. Adamo, C. Amatore, I. Ciofini, A. Jutand, H. Lakmini, *J. Am. Chem. Soc.* **2006**, *128*, 6829–6836; b) H. Lakmini, I. Ciofini, A. Jutand, C. Amatore, C. Adamo, *J. Phys. Chem. A* **2008**, *112*, 12896–12903.

[10] For the synthesis of *trans*-$[ArPdX(PPh_3)_2]$ (X = I, Br, Cl), see: P. Fitton, E. A. Rick, *J. Organomet. Chem.* **1971**, *28*, 287–291.

[11] For a review on the use of electrochemical techniques to investigate the mechanisms of transition metal-catalyzed reactions, see: A. Jutand, *Chem. Rev.* **2008**, *108*, 2300–2347.

[12] C. Amatore, A. Jutand, F. Khalil, M. A. M'Barki, L. Mottier, *Organometallics* **1993**, *12*, 3168–3178.

[13] a) C. Amatore, A. Jutand, F. Khalil, M. F. Nielsen, *J. Am. Chem. Soc.* **1992**, *114*, 7076–7085; b) C. Amatore, E. Carré, A. Jutand, H. Tanaka, R. Quinghua, S. Torii, *Chem. Eur. J.* **1996**, *2*, 957–966.

[14] a) M. J. S. Dewar, R. Jones, *J. Am. Chem. Soc.* **1967**, *89*, 2408–2410; b) A. N. Cammidge, V. H. M. Goddard, H. Gopee, N. L. Harrison, D. L. Hughes, C. J. Schubert, B. M. Sutton, G. L. Watts, A. J. Whitehead, *Org. Lett.* **2006**, *8*, 4071–4074.

[15] V. V. Grushin, H. Alper, *Organometallics* **1993**, *12*, 1890–1901.

[16] a) *trans*-[(Ph)Pd(OH)$(PPh_3)_2$] formed by addition of excess PPh_3 to a *cis*/*trans* mixture of [{(Ph)Pd(μ-OH)(PPh_3)}$_2$] (Scheme 8) could not be isolated from most investigated solvents (DMF not tested), as reported by Grushin and Alper. However, its ^{31}P NMR signal has been observed in CD_2Cl_2 ($\delta=23.3$ ppm, 18 °C). See: V. V. Grushin, H. Alper, *Organometallics* **1996**, *15*, 5242–5245; b) it has been verified by ^{31}P NMR spectroscopy that under our experimental conditions ($[PPh_3]=5.7$ mM and [{(Ph)Pd(μ-OH)(PPh_3)}$_2$] = 0.95 mM), the formation of *trans*-[(Ph)Pd(OH)$(PPh_3)_2$] is quantitative; c) the dimer [{ArPd(μ-OH)(PPh_3)}$_2$] is not involved in the reaction of *trans*-$[ArPdBr(PPh_3)_2]$ (Ar = *p*-NC-C_6H_4; $C_0=1.9$ mM) with $PhB(OH)_2$ (20 equiv) in the presence of OH^- (16.7 equiv). Indeed, the same value of k_{obs} was determined when two reactions were per-

formed in the presence of different amounts of PPh_3 (2 and 10 equiv), indicating that the equilibrium between the dimer and *trans*-[ArPd(OH)(PPh_3)$_2$] was fully shifted towards the latter in the presence of at least 2 equivalents of PPh_3 with respect to the initial Pd^{II} complex.

[17] For the detection of stable [ArPdAr′(PPh_3)$_2$] (Ar = pyridyl, Ar′ = Ph, *o*-tolyl, mesityl) in Pd-catalyzed Suzuki–Miyaura reactions by ESI MS, see: A. O. Aliprantis, J. W. Canary, *J. Am. Chem. Soc.* **1994**, *116*, 6985–6986.

[18] Since OH^- was introduced from a 1 M solution of nBu_4NOH in methanol, it was checked that the addition of methanol (200 μL) did not affect the stability of *trans*-[(Ph)Pd(Ph)(PPh_3)$_2$].

[19] For the formation of anionic pentacoordinated Pd^{II} species, see: C. Amatore, A. Jutand, *Acc. Chem. Res.* **2000**, *33*, 314–321.

[20] For reductive elimination induced by a fifth ligand on square-planar d^{10} complexes, see: a) R. Giovannini, P. Knochel, *J. Am. Chem. Soc.* **1998**, *120*, 11186–11187; b) F. d'Orlyé, A. Jutand, *Tetrahedron* **2005**, *61*, 9670–9678.

[21] a) The kinetics of the formation of [$Pd^0(PPh_3)_3$] in the reaction of *p*-MeO-C_6H_4-$B(OH)_2$ with *trans*-[(Ph)PdBr(PPh_3)$_2$] (1.9 mM) in the presence of PPh_3 (2 equiv) and OH^- was investigated. The reactions were quite fast ($t_{1/2}$ = 7.5 s when β = 20 and α = 10; $t_{1/2}$ = 10 s when β = 20 and α = 15, $t_{1/2}$ = 7.5 s when β = 10 and α = 5). These timescales are considerably shorter than that observed for the reductive elimination performed from the intermediate complex *trans*-[(*p*-MeO-C_6H_4)Pd(Ph)(PPh_3)$_2$] in the absence of OH^- (see text); b) moreover, the kinetic curves obtained in the presence of OH^- were not S-shaped and were affected by the concentrations of *p*-MeO-C_6H_4-$B(OH)_2$ and OH^-. Consequently, these kinetic curves did not characterize the reductive elimination (which should be zero-order for Ar′$B(OH)_2$), but rather the rate-determining transmetalation followed by a faster reductive elimination.

[22] For an illustration of the oxophilicity of arylboronic acids with [Rh–OH] complexes, see: a) A. Kina, H. Iwamura, T. Hayashi, *J. Am. Chem. Soc.* **2006**, *128*, 3904–3905; b) P. Zhao, C. D. Incarvito, J. F. Hartwig, *J. Am. Chem. Soc.* **2007**, *129*, 1876–1877.

[23] G. Espino, A. Kurbangalieva, J. M. Brown, *Chem. Commun.* **2007**, 1742–1744.

[24] When Z′ = CN, the increase in the [$Pd^0(PPh_3)_3$] concentration was not strictly exponential as the value of the oxidation current of [$Pd^0(PPh_3)_3$] did not reach a constant final value. However, voltammograms acquired by oxidation and then reduction at the "end" of the reaction revealed the formation of [$Pd^0(PPh_3)_3$] and *p*-NC-C_6H_4-C_6H_4-*p*-CN in high yields (Table 1), indicative of a real reaction, the k_{obs} of which could not, however, be determined by the application of a simple logarithmic rate law.

[25] The reactions were not tested when Z = Me or MeO because of the instability of the corresponding *trans*-[ArPdX(PPh_3)$_2$] complexes due to slow ligand scrambling between the Ar group and the Ph groups of the phosphine.

[26] The same order was established for the substitution of X^- by OAc^- in [(Ph)PdX(PPh_3)$_2$] in DMF.[6b]

[27] a) General rate law according to the mechanism outlined in Scheme 12:
rate = k_{tm}[Ar′$B(OH)_2$][ArPd(OH)L_2] with:

$$[Ar'B(OH)_2] = \frac{\beta C_0}{1+K_{OH}[OH^-]} \quad \text{and} \quad [ArPd(OH)L_2] = K_X \frac{[OH^-][ArPdXL_2]}{[X^-]}$$

in which $[Ar'B(OH)_2]_0 = \beta C_0$, which was in excess ($\beta > 10$ in our conditions). On the other hand, the total Pd^{II} concentration is given by:

$$\left[Pd^{II}\right]_{total} = [ArPdXL_2] + [ArPd(OH)L_2] =$$

$$[ArPd(OH)L_2]\left(1 + \frac{[X^-]}{K_X[OH^-]}\right)$$

Since the measured rate constant k_{obs} referred to the total amount of Pd^{II}, the rate is given by:

$$\text{rate} = k_{obs}\left[Pd^{II}\right]_{total} = k_{tm}\beta C_0 \times \frac{1}{1+K_{OH}[OH^-]} \times \frac{K_X[OH^-]}{[X^-]+K_X[OH^-]}\left[Pd^{II}\right]_{total}$$

$d\left[Pd^{II}\right]/dt = -k_{obs}\left[Pd^{II}\right]$, after integration, one has: $\ln x = -k_{obs}t$

$$k_{obs} = \frac{k_{tm}\beta C_0[OH^-]}{K_X K_{OH}[OH^-]^2 + (K_X + K_{OH}[X^-])[OH^-] + [X^-]} = \frac{A[OH^-]}{a[OH^-]^2 + b[OH^-] + c}$$

Noting $A = k_{tm}K_X\beta C_0; a = K_X K_{OH}; b = K_X + K_{OH}[X^-]; c = [X^-]$, the derivative of k_{obs} versus $[OH^-]$ is given by:

$$D = \frac{A\left(c - a[OH^-]^2\right)}{\left(a[OH^-]^2 + b[OH^-] + c\right)^2}$$

which is null when $[OH^-]_{max} = (c/a)^{1/2} = ([X^-]/K_X K_{OH})^{1/2}$. b) Hence, pure pseudo-first-order kinetics (viz., $k_{obs} \approx$ constant) associated with a pure exponential decay of $[Pd^{II}]$ may be observed only when the above conditions on α, β, and $(\beta-\alpha)$ are fulfilled, as well as $K_X[OH^-] \gg C_0$, this latter inequality being required for the variations in $[X^-]$ to have no significant influence on the value of k_{obs}. When this is not strictly the case, k_{obs} is expected to vary slightly along the reaction course, reflecting the variations in $[X^-]$ and $[OH^-]$. Experimentally, this is expected to introduce some oscillation of the instantaneous slope of the concentration–time variations around a mean value (compare to Figure 1e).

[28] If the selected initial concentration of OH^- is too high ($\alpha \gg \beta$), the reaction will not proceed due to exclusive formation of the unreactive Ar′$B(OH)_3^-$. This is reflected in the kinetic laws derived above (see text and footnote [27]) by the appearance of the term $(\beta-\alpha)$ in several expressions.

[29] It is also of interest to note that the maximum of the bell-shaped variations of $k_{obs\,(50\%)}$ may be rather flat when the conditions $[OH^-] \gg 1/K_{OH}$ and $[OH^-] \gg C_0/(2K_X)$ are met separately, as observed, for example, in Figure 2a, since there is then a rather large intermediate zone between the ranges of α/β values in which both of the above limits may apply (compare Figures 2a or 4b,c).

[30] Such a result justifies a posteriori that the expressions for k_{obs} in Equations (2) and (3) are almost constant as soon as $(\beta-\alpha) \gg 1$, thereby validating that near-exponential productions of Pd^0 with time were observed (Figure 1e).

[31] The situation to which a given experiment conforms is mostly dictated by the value of the ratio α/β, which, in turn, is imposed by K_X and K_{OH}, α and β. For the system at hand, however, the role of these latter parameters is minimal because $K_{OH}/K_X \gg 1\,M^{-1}$.

[32] Note that for the sake of simplicity, the formulation "Pd^0L_2" is used in Scheme 13 instead of the more appropriate [Pd^0L_2X]$^-$.[19]

Received: July 6, 2010
Revised: October 14, 2010
Published online: January 17, 2011

